Carbohydrate Polymers 86 (2011) 1565–1572

Contents lists available at ScienceDirect

Carbohydrate Polymers

journal homepage: www.elsevier.com/locate/carbpol

Ceramic membrane filtration for isolating starch nanocrystals

Déborah LeCorre, Julien Bras, Alain Dufresne*

The International School of Paper, Print Media and Biomaterials (Pagora), Grenoble Institute of Technology, BP 65 - F-38402 Saint Martin d'Hères Cedex, France

ARTICLE INFO

Article history:
Received 18 May 2011
Received in revised form 17 June 2011
Accepted 21 June 2011
Available online 30 June 2011

Keywords:
Starch
Nanocrystals
Microfiltration
Membrane

ABSTRACT

Starch nanocrystals (SNC) present different sizes (microscale and nanoscale) limiting their yield, process parameters and properties. Therefore, hydrolysates from wheat starch were filtered using a microfiltration unit equipped with ceramic membranes to assess the cross-flow membrane filtration potential of SNC suspensions. Properties of feed, permeate and retentate were evaluated with dynamic light scattering, SEM, SEM-FEG and X-ray diffraction. Process parameters were also monitored. Achieved permeate flux was 306–510 $dm^3\ h^{-1}\ m^{-2}$ depending on membrane pore size and transmembrane pressure. Volume concentration ratio reached 13.7. Results show that microfiltration can be a promising solution to achieve separation of nanocrystals from non-fully hydrolyzed particles. No significant differences in final particles size were observed for all tested membranes. Analysis on permeate shows not only that collected nanoparticles are more crystalline than feed, but also that mostly B-type particles are produced during the first day of hydrolysis. These very promising results completely change the way of thinking with respect to SNC preparation.

1. Introduction

These last decades an important concept has been brought up by scientists for the development of new products, i.e. the need for more efficient and less environmentally impacting materials. It has brought two scientific fields together: (i) nanotechnologies which allow the development of innovative and efficient materials, and (ii) biomaterials processing with the use of renewable raw materials for more environmentally friendly and sustainable solutions. Due to their semi-crystalline structure polysaccharides offer the opportunity to integrate these two fields by producing bionanoparticles.

Starch nanocrystals (SNC) are candidates of growing interest. They are crystalline platelets resulting from the disruption of the semi-crystalline structure of starch granules by the hydrolysis of amorphous parts. Their preparation by acid hydrolysis has been optimized a few years ago (Angellier, Choisnard, Molina-Boisseau, Ozil, & Dufresne, 2004) and very promising mechanical and barrier properties have been reported when used in nanocomposite applications (Angellier, Molina-Boisseau, & Dufresne, 2005a; Angellier, Molina-Boisseau, Lebrun, & Dufresne, 2005b; Angellier, Putaux, Molina-Boisseau, Dupeyre, & Dufresne, 2005c; Angellier, Molina-Boisseau, Dole, & Dufresne, 2006a; Angellier, Molina-Boisseau, & Dufresne, 2006b; Chen et al., 2008a; Chen, Cao, Chang, & Huneault, 2008b; Kristo & Biliaderis, 2007; Viguié, Molina-Boisseau, & Dufresne, 2007). For these reasons, SNC are being studied in detail for example in a recent European Project (FlexPakRenew–FP7/2007-2013 – no. 207810) and reviews have recently been published (LeCorre, Bras, & Dufresne, 2010; Lin, Huang, Chang, Anderson, & Yu, 2011).

The main challenges for the development and use of SNC have only very recently been clearly identified. They are twofold. The first one relates to the production scale. Indeed, the current protocol applies for producing small quantities of SNC (250 mL) and renders a limited yield (10–15%) after a long production time (5 days). The second challenge deals with the hydrolysis of starch with respect to its onion-like structure. A very recent study (LeCorre, Bras, & Dufresne, 2011) showed for the first time that resulting SNC suspension contains both micro and nanoparticles whatever the extent of hydrolysis. It was also proved that SNC were already present in the suspensions after only 24 h hydrolysis.

A way of overcoming these two issues would be to identify a process for extracting SNC during the hydrolysis process. First trials using differential centrifugation have been unsuccessful (LeCorre et al., 2011) leading to the need of investigation of a continuous extraction technique, viz. cross-flow membrane filtration. The aim is to assess the possibility of separating SNC from microparticles in a continuous flow.

Membrane separation processes driven by pressure, like microfiltration (MF) have aimed at the purification of diluted solutions with low concentration of solid and dissolved particles (Hinkova,

* Corresponding author. Tel.: +33 4 76 82 69 95; fax: +33 4 76 82 69 95.
E-mail address: Alain.Dufresne@pagora.grenoble-inp.fr (A. Dufresne).

0144-8617/$ – see front matter © 2011 Elsevier Ltd. All rights reserved.
doi:10.1016/j.carbpol.2011.06.064

Bohacenko, Bubnik, Hrstkova, & Jankovska, 2004). Ultrafiltration membranes, characterized by a mean pore size of 10^{-3} to 10^{-1} μm, find numerous applications nowadays. The starch industry for example pays great attention to the refinement of raw starch syrups after starch hydrolysis and to their wastewater treatment (Pidgeon, 2009). Also, (Singh & Cheryan, 1997; Singh & Cheryan, 1998a; Singh & Cheryan, 1998b) in comparison with rotary vacuum filtration membrane processes were found more economical and more effective. This statement led us to investigate the use of such processes to filter slightly bigger particles formerly known as starch hydrolysate insoluble residues and more recently identified as SNC suspensions.

The idea was to check if the progressive "release" of SNC can be considered as an advantage to increase the production yield. Their continuous extraction during hydrolysis should strongly increase the quantity and the homogeneity of particles and could be a clear breakthrough in the field. To that purpose, cross-flow (tangential) filtration appeared most appropriate. Microfiltration membrane with pore size 10^{-1} to 1 μm and wheat starch, which hydrolysate has been reported to have much lower filtration rate (Master & Steeneken, 1998), have been selected to assess the membrane filtration potential of SNC.

2. Materials and methods

2.1. Materials

Wheat starch (Cerestar PT 20002) was kindly provided by Cargill (Krefeld, Germany). Theoretical amylose content was 28%. Sulfuric acid was purchased at 96–99% purity from Sigma Aldrich and was used after dilution at 3.16 M with distilled water.

2.1.1. Starch nanocrystals suspension

Wheat starch was hydrolyzed during one day, adapting the previously described optimized procedure (Angellier et al., 2004) for producing SNC. Wheat starch (147 g) was mixed with 1 L of previously prepared diluted sulfuric acid (3 M). The suspension was kept under 400 rpm mechanical stirring at 40 °C, using a silicon oil bath for 5 days. The final suspension was washed by successive centrifugation *(Centrifuge 6K-15C, Sigma)* at 10,000 rpm (RCF = 16,211 g) in distilled water until reaching neutral pH, and redispersed using Ultra Turrax for 5 min at 13,000 rpm to avoid aggregates. To provide sufficient amount (20 L) for the pilot run, the final suspension was diluted. The final concentration was 0.5 wt%.

2.1.2. Microfiltration

A XLAB4 cross-flow pilot unit (Pall, France) was equipped with four ceramic membranes Membralox (Module T1-70) having mean pore size of 0.1, 0.2, 0.5 and 0.8 μm, as shown in Fig. 1. The pilot was equipped with two parallel channels, each containing 2 membranes, the first one being submitted to higher pressure. After pre-trials performed in closed loop or recycled mode (VCF = 1) at transmembrane pressure (TMP) 60 and 100 kPa, filtration experiment was performed for the same TMPs but the permeate was collected for analysis. Cross-flow velocity was 5 m s^{-1}. The pH was neutral or slightly acidic and temperature was 25 °C.

2.1.3. Filtration parameters

The volume concentration ratio (VCR) corresponds to the ratio of the feed volume to the volume of the retentate. It is commonly used in the industry to assess the concentration power of a filtration process. A VCR value of 1 implies that there was no concentration and hence the experiment was performed in total recycled mode (Singh & Cheryan, 1998b). In this study, VCR was assessed for the pilot containing the four membranes and not for each membrane.

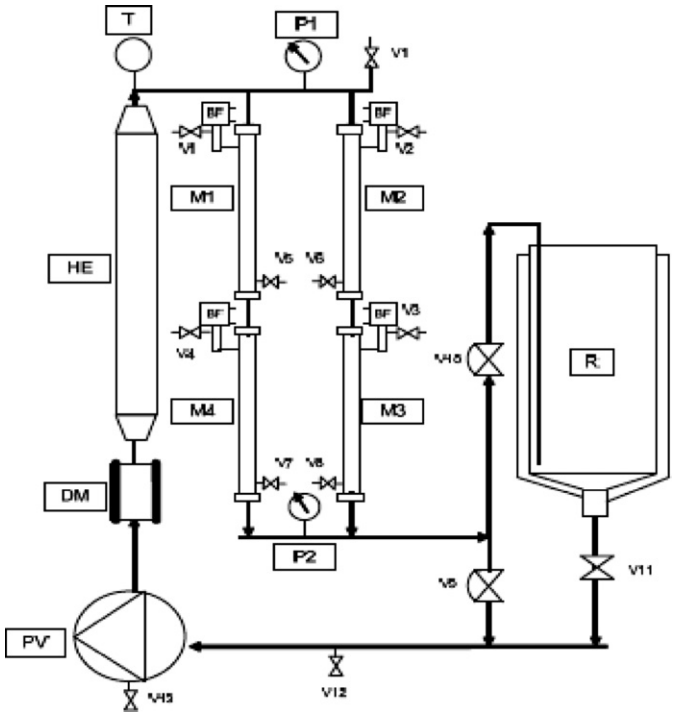

Fig. 1. XLAB4 Pilot unit. M1: membrane 0.1 μm. M2: membrane 0.2 μm. M3: membrane 0.5 μm. M4: membrane 0.8 μm.

The permeate flux ($J_{P,t}$) is expressed in $dm^3\ h^{-1}\ m^{-2}$ according to:

$$J_{P,t} = \frac{V_p}{A_f \times t} \quad (1)$$

where V_p is the volume of permeate (L), A_f is the filtration area (m^2) and t is time (h).

The reduction of permeate flux (ΔJ) is calculated from:

$$\Delta J = \frac{J_{P,0} - J_{P,t}}{J_{P,0}} \times 100 \quad (2)$$

where $J_{P,0}$ is the permeate flux at $t = 0$ s and $J_{P,t}$ is the permeate flux at time t.

The transmembrane pressure (TMP) is the pressure drop across the membrane. It is calculated according to:

$$\mathrm{TMP} = \frac{P_f + P_r}{2} - P_p \quad (3)$$

with P_f, P_r and P_p being the feed, retentate and permeate pressure, respectively (Kumar, Madhu, & Roy, 2007). The membrane fouling model parameters, k and J_{ss}, correspond to the fouling rate and the steady state permeate flux, respectively, both expressed in $L\ h^{-1}\ m^{-2}$. They can be calculated by fitting experimental values to equation:

$$J_{P,t} = J_{ss} + Kt^{-1} \quad (4)$$

2.1.4. Microscopies

An environmental scanning electron microscopy (ESEM) on a Quanta 200 FEI device (Everhart-Thornley Detector) was used at high voltage (10 kV) to access the morphology of native starches. Native starches were simply deposited onto carbon tape before observation.

SNC' mean size and morphology were studied using a Zeiss Ultra 55 Field Emission Gun Scanning Electron Microscope (FEG-SEM). A thin Au–Pd conductive coating (~1 nm) was performed to reduce charge effect. The images obtained at 10 kV accelerating voltage and working distance of 8–10 mm lead to the best compromise in

terms of SNC contrast and residual charge effect. In order to obtain the best possible resolution, the secondary electron imaging mode with the in-lens detector was used.

2.1.5. Particle size measurements

Particle size measurements were performed at 25 °C with a commercial Zeta-sizer (Zetasizer NanoZS, Malvern, France). The particle radii were controlled by light scattering. For each measurement, the suspension was diluted to a concentration of 0.01 wt%. Then a given volume of the diluted solution was injected in the Zetasizer cell after 30 s homogenization with ultrasonic bath. The size was measured after reaching stable values.

2.1.6. X-ray diffraction

The wide angle X-ray diffraction analysis was performed on powders obtained from either native starch or air-dried SNC suspensions conditioned at temperate conditions (23 °C, 50% RH). Measurements were then carried out at room temperature (23 °C) and relative humidity (28.8%). The samples were placed in a 2.5 mm deep cell and measurements were performed with a PANanalytical, X'Pert PRO MPD diffractometer equipped with an X'celerator detector. The operating conditions for the refractometer were: Copper Kα radiation, 2θ between 4 and 44°, step size 0.067°, and counting time 90 s.

3. Results and discussion

3.1. Filtration process

The main objective of this experiment was to extract SNC from the hydrolysate suspensions as soon as they are produced. Fig. 2 summarizes this strategy. It is based on results from a very recent study proving the existence of SNC in the suspension after only 1 day (LeCorre et al., 2011). Cross-flow microfiltration was the selected process for limiting the conversion of SNC into oligo or monosaccharides. For such an extraction to be possible, the system has to be acid-proof, hence the use of a ceramic membrane. However, the whole filtration unit, including pipes, pumps and containers should be acid-resistant as well in our conditions. Acidic conditions for the production of SNC are quite strong (3.16 M H_2SO_4) compared to acidic conditions found in the industry (max. 5% HCl or 1.3 M HCl). To our knowledge, no such filtration unit has been developed. Therefore, we used a regular pilot unit (Fig. 1) with neutralized 1-day-hydrolyzed-starch suspension (quenched) as a proof of principle. Pre-trials were performed in recycled mode (VCR = 1) to assess the membrane behavior under different transmembrane pressure (TMP) being 60 and 100 kPa as it has been reported that for starch hydrolysate and syrups TMP higher than 103 kPa did not improve flux (Singh & Cheryan, 1997). Recommended cross-flow velocity was also relatively high (5 m s^{-1}) as increasing cross-flow velocity is probably the easiest way to reduce fouling and maximize flux during microfiltration of corn starch hydrolysate (Singh & Cheryan, 1997).

3.2. Filtration kinetics

The filtration kinetics was investigated for all four membranes during all the experiment. Experimental data are reported in Table 1 No correlation was observed between decrease in permeate flux and membrane pore size due to large variations observed in Fig. 3(a). However, reported permeate flux at low TMP (<100 kPa) and low temperature (25 °C) are high (300–600 L m^{-2} h^{-1}) compared to data reported in other studies. For the filtration of corn starch hydrolysate at same cross-flow velocity (5 m s^{-1}), reported flux were 100–180 L m^{-2} h^{-1} (Hinkova et al., 2004; Singh & Cheryan, 1997) for TMP = 100–1000 kPa and T = 40–60 °C.

Fig. 3 shows the evolution of the permeate flux during filtration on membranes with different pore sizes. For all membranes, the permeate flux oscillates strongly but following a declining slope. These oscillations are possibly linked to (i) the heterogeneity of the suspension, (ii) the measurement method and/or (iii) the possible fouling that can occur during the microfiltration process. Membrane fouling is generally due to the accumulation of submicron particles on the membrane surface and within the pores of the membrane itself. The former effect is called concentration polarization. It results from the reversible accumulation of the rejected solute in the fluid phase at the membrane-fluid interface as the solvent phase passes through the membrane. However, if steady state prevails, the solute retained will be transported back into the bulk solution through the boundary layer because of the concentration difference (Cheryan, 1986). Internal fouling (clogging) of the pores of an asymmetric membrane, however, is very rare (GmbH) and results in an irreversible decline in the flux with time. Concentration polarization effects can be reduced by decreasing the transmembrane pressure or lowering the feed concentration. According to Singh and Cheryan (1997), the best model for describing the fouling process is given by Eq. (4). The steady state flux, J_{ss}, and fouling rate, k, should be correlated with operating parameters.

These parameters calculated from the fouling model and reported in Table 1 allowed for drawing the declining slope as shown in Fig. 3b. It seems that the small the pore size, the higher the fouling rate (Table 1). Indeed, if the pore diameter is smaller than the largest particles, the pores will be plugged and prevent smaller particles to pass through the membrane. In this study, all membranes have pore sizes smaller than the largest particles. However, the smaller the membrane pore size, the more numerous the particles larger than pore size. Thus, smaller pore size membranes have a higher fouling rate. It should, nevertheless, be noted that the higher the pore size of the membrane, the lower the correlation with the fouling model as indicated by the values of the coefficient of determination R^2 reported in Table 1. It suggests that reported flux have not reached steady state and that fouling has not completely occurred. However, this gradual decrease in flux is characteristic of membrane fouling which decreases the efficiency of the filtration process. The experiment lasted over 2.5 h and could not be extended. Indeed, it reached maximum VCR for this pilot (13.6) before observing fouling. This was expected as the experiment was carried out on a 24 h hydrolyzed starch suspension therefore containing a majority of microscopic particles and a few nanometer scale particles. In a continuous process, retentate would be recycled back to the hydrolysis tank. Nevertheless, the loss in permeate flux was relatively moderate (20–40%).

Contrary to what was expected the filtration kinetics and fouling does not seem to be correlated to the pore size of the membrane. Strong fluctuations in flux make it difficult to appoint the best pore size for this application. Indeed, membrane 0.2 μm renders the most stable flux, while membrane 0.5 μm renders the highest flux and membrane 0.8 μm renders the smallest reduction in permeate flux. It seems that the pore size of the membrane is not a governing factor for our filtration process. Indeed, the performance of the membrane filtration and fouling mechanism depends on various factors such as the operating conditions of the system (including filtration pressure, cross-flow velocity, soluble microbial products (SMP) concentration, etc.) and the membrane characteristics (morphology, membrane pore size, zeta potential, hydrophilic affinity, etc.), but also the nature of biological polymers and bio-macromolecular characteristics (molecular weight of biopolymers, zeta potential, configuration, size distribution, etc.) (Hwang & Huang, 2009). These last sets of parameters probably apply to SNC suspensions. However, despite instability, microfiltration worked efficiently to isolate SNC from microparticles whichever the membrane.

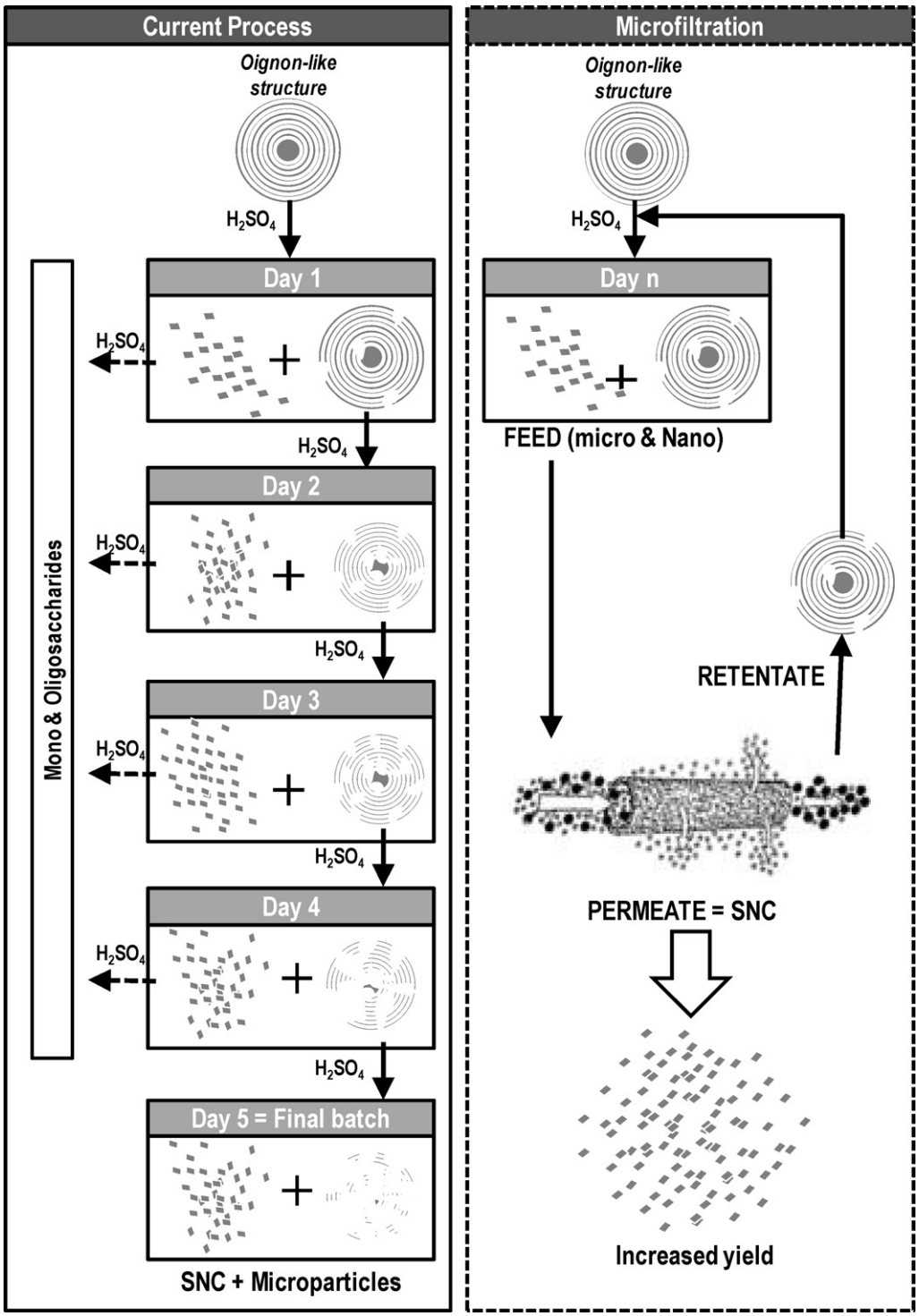

Fig. 2. Schematic comparison between the current preparation process involving the progressive production of starch nanocrystals as evidenced in (LeCorre et al., 2011), and the proposed microfiltration process.

Table 1
Summary of the filtration kinetics data (permeate flux) and coefficients of fouling model for microfiltration of wheat starch nanocrystals at 25 °C, 5 m s^{-1}, neutral pH.

Membrane pore size		0.1 μm	0.2 μm	0.5 μm	0.8 μm
TMP (kPa)		100	100	60	60
Inital permeate flux ($dm^3\ h^{-1}\ m^{-2}$)	t = 0 h	480	587	413	293
Final permeate flux ($dm^3\ h^{-1}\ m^{-2}$)	t = 2 h 40 min	320	360	240	231
Relative reduction of permeate flux ΔJ_p (%)		33.3%	38.7%	41.9%	21.2%
Steady state permeate flux ($dm^3\ h^{-1}\ m^{-2}$)	J_{ss}	313	411	279	210
Fouling rate ($dm^3\ h^{-1}\ m^{-2}$)	k	29	31	23	13
Determination coefficient	R^2	0.82	0.66	0.45	0.27

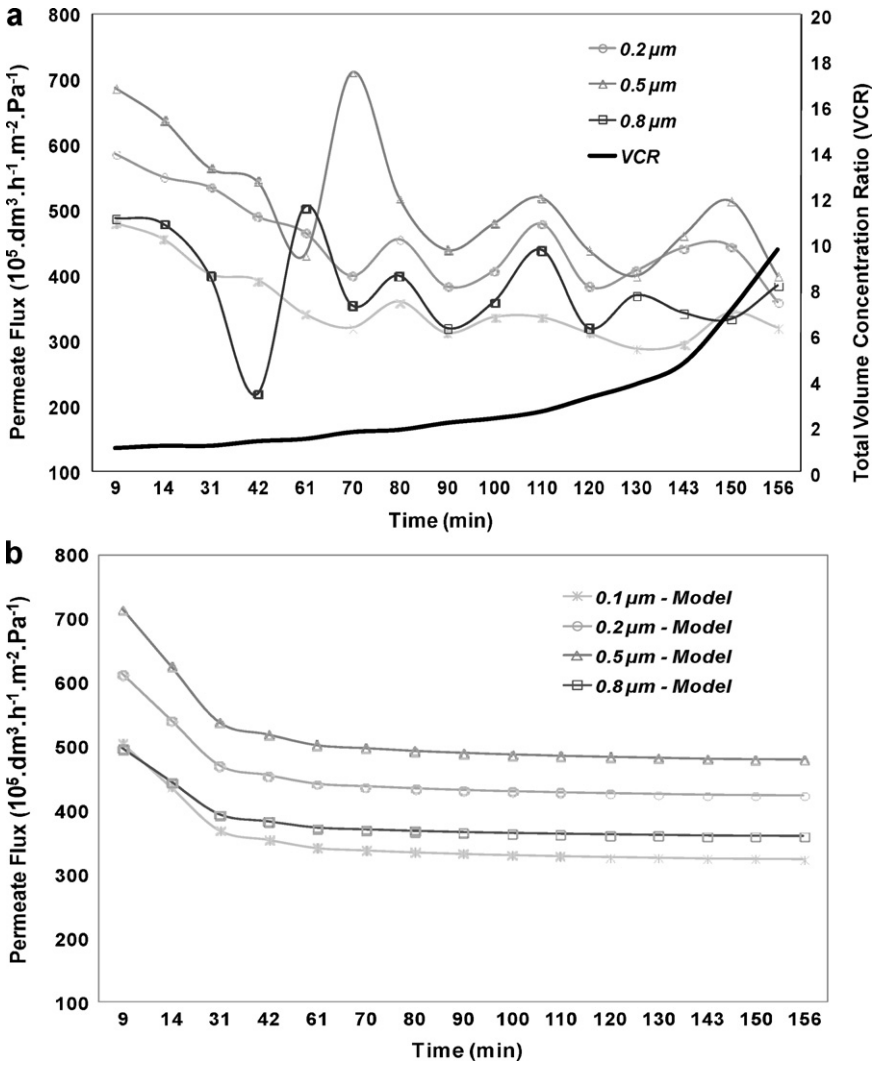

Fig. 3. Evolution of the permeate flux during filtration through membranes with different pore sizes (0.1 μm, 0.2 μm, 0.5 μm, and 0.8 μm): (a) actual oscillations, (b) modeling with fouling parameters.

3.3. Collected suspensions properties

Dynamic light scattering was used to assess differences in size among suspensions filtrated with the four different pore size ceramic membranes and between the initial suspension and the final retentate. Experimental data are collected in Table 2. The high polydispersity index (PdI, ratio between width and magnitude of the size peaks) indicates a relatively broad size distribution and implies that *Z*-average size cannot be reported for comparison with other devices. Despite that, clear differences in size were observed between particles contained in the feed, retentate and permeate, as shown in Fig. 4a. The mean particle size for the feed suspension was estimated at 800 nm (100 number %) whereas it was much smaller for the permeate (~100 nm depending on membrane) and much bigger for the retentate (1255 nm) as expected. Indeed, the latter is made of particles that cannot pass through the membrane. However, higher values were expected as native wheat starch granules are 2–30 μm and are not likely to all be hydrolyzed down to 1 μm after only 1 day. An explanation could be that biggest particles undergo shear stress during fouling or precipitate to the bottom before being measured by the diffractive laser.

Finally, permeates coming from the different filtrations were compared. They all exhibited a bimodal distribution with a main peak at 50–100 nm and a secondary peak at 200–400 nm. The secondary peak was attributed to the presence of aggregates that either passed through the ceramic membrane or formed after filtration. No significant differences were observed among permeate size obtained with membranes with different pore sizes. After 1 day hydrolysis, a membrane with pore size 0.8 μm seems enough to be efficient to discriminate granules from SNC. As it is also the membrane for which the lowest loss of permeate flux and lowest fouling was observed (Fig. 1), it should be selected for future test runs. Indeed, membrane replacement accounts for about 55% of the operating costs of a ceramic membrane plant (Singh & Cheryan, 1998b). Also, potential flux improvement and further fouling reduction can be expected if cross-flow velocity is increased (Singh & Cheryan, 1997). Thus, we recommend selecting the cheapest membrane (larger pore size) and increasing cross-flow filtration for a cost effective application of this process.

SEM micrographs of the suspensions were taken to control visually the content of each suspension. As expected from wheat starch granules and giving particle size analysis, the feed suspension is made of disc-like particles and a few smaller round particles as seen in Fig. 4b. Biggest particles (granules) have also been attacked by acid as pit holes can be seen at the surface. However, SNC cannot be observed with regular ESEM at this magnitude. Fig. 4b also shows that particles from the retentate seem to have been

Table 2
Summary of dynamic light scattering data for feed, retentate and permeate. PdI: polydispersity index. % number reflects the distribution of particles among the first and the second peak.

Sample type	Main peak		Secondary peak		PdI
	Mean particle size (nm)	% Number	Mean particle size (nm)	% Number	
Feed	804 ± 205	100%			0.58 ± 0.21
Retentate	1255 ± 318	100%			0.38 ± 0.66
Permeate 0.8 μm	51 ± 7	99% ± 0,2%	211 ± 46	1% ± 0,2%	0.77 ± 0.06
Permeate 0.5 μm	122 ± 13	13% ± 3%	480 ± 63	87% ± 3%	0.55 ± 0.05
Permeate 0.2 μm	71 ± 2	99% ± 28%	362 ± 101	1% ± 28%	0.74 ± 0.24
Permeate 0.1 μm	Not repeatable measurement				

roughly grounded. That is most likely due to the pressure applied to particles during membrane fouling, submitting them to shear stress.

FEG-SEM micrographs of the permeate show SNC of about 50 nm (Fig. 5a) and re-aggregates of particles of about 200 nm (Fig. 5b) as well as non-fully individualized nanocrytals of about 500 nm (Fig. 5c). These results confirm the dimension analysis from Table 2 and prove that cross-flow filtration is a promising solution for separating SNC from non-fully acid hydrolyzed starch granules. This is the first time that such a possibility is proposed for this application. However, it was important to prove that such a process, with the mechanical stress which may result from filtration and polarization, did not alter the structure of SNC.

For this reason, X-ray diffraction (XRD) measurements were used to assess the crystallinity of particles in each suspension. Fig. 6 shows the X-ray diffraction patterns obtained for the feed suspension of 24-h-hydrolyzed starch, as well as for the permeate and retentate of that same suspension after microfiltration on a 0.8 μm pore size ceramic membrane. As expected, the initially freeze-dried feed suspension rendered an A-type diffraction pattern with strong reflection peaks at 2θ values around 15° and 23° and an unresolved doublet at 17° and 18° as well as two weak peaks around 2θ values around 10° and 11°. Compared to the feed suspension, no significant difference was observed for the retentate. On the contrary, the diffractogram for the permeate suspension revealed two significant differences. First, sharper XRD patterns consistent with a higher level of crystallinity were observed. Calculations from this data reveal an increase of 3.5% in crystallinity from 34.6% to 38.2% for feed and permeate, respectively. Second, crystalline peaks seem to be characteristic of a B-type starch with the strongest diffraction peak at around 2θ value of 17° and a few smaller peaks at 20°, 22° and 23° and an additional peak which appeared at about 5°.

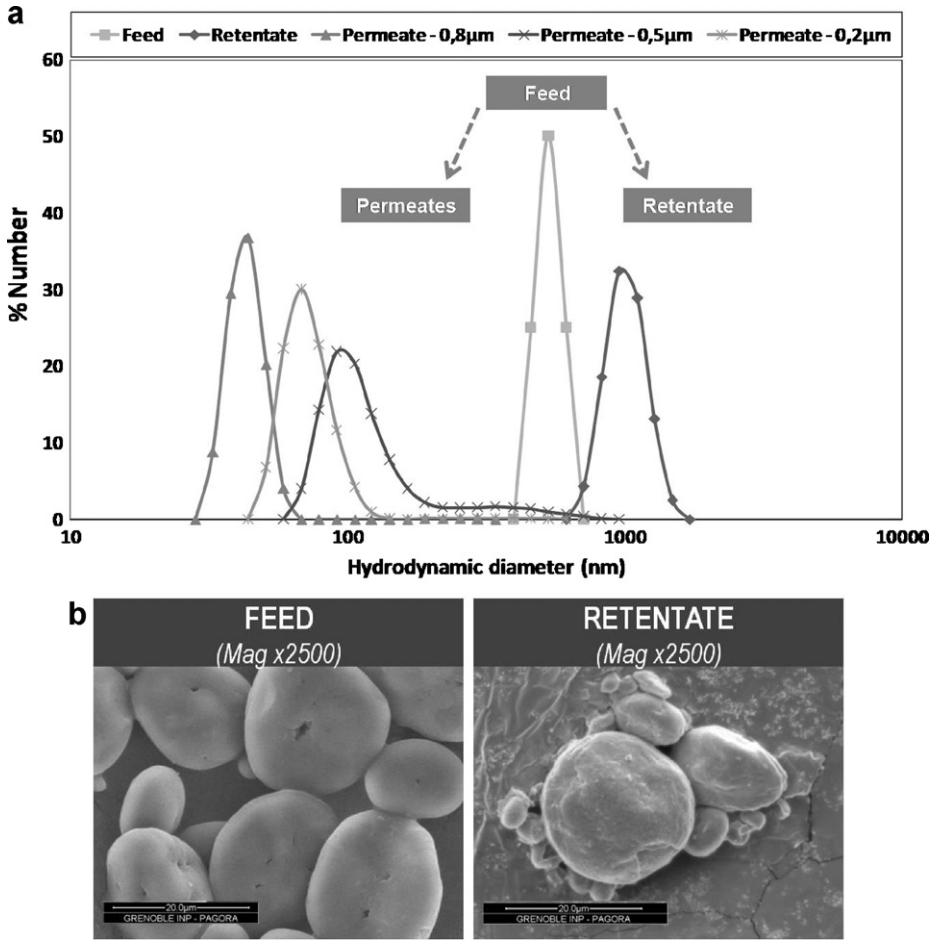

Fig. 4. (a) Particle size distribution of feed, retentate and permeate suspensions determined from dynamic light scattering experiments, and (b) ESEM micrographs of 1-day-acid-hydrolysis feed suspension and retentate suspension at magnitude 2500×.

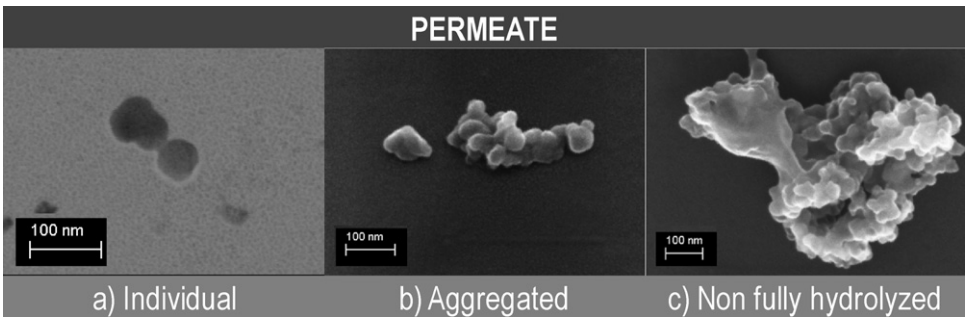

Fig. 5. FEG-SEM micrographs of the 1-day-acid-hydrolysis permeate suspension: (a) individual nanocrystals in transmission mode, (b) re-aggregated particles in reflective mode, (c) non-fully individualized particles in reflection mode.

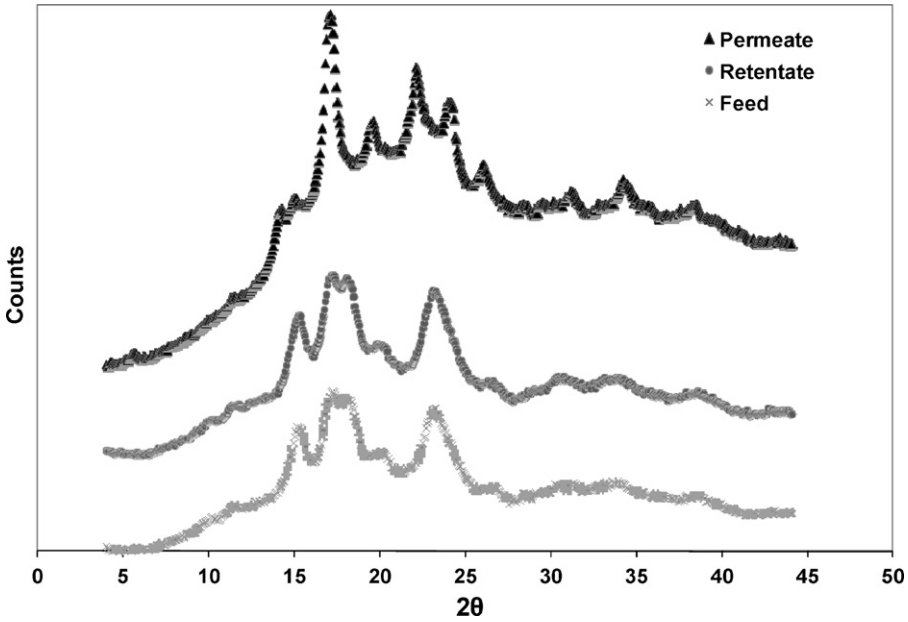

Fig. 6. X-ray diffraction patterns of the feed suspension, retentate and permeate (obtained through the 0.8 μm membrane).

The first difference can be easily explained, as we believe to have collected in permeate, SNC produced after 24 h hydrolysis. The second difference can be attributed to the fact that wheat starch granules consist of two populations, i.e. one of small (1–10 μm) spherical B-type granules and a second of bigger (15–40 μm) disc-shaped A-type granules. As reported by Jane, Wong, & McPherson (1997), contrary to A-type starch which branch linkages might be protected in the crystalline region, B-type starch has most amylopectin branch points clustered in the amorphous region, making it more susceptible to acid hydrolysis. It is most likely that B-type crystallites are produced more quickly (i.e. after one day) than A-type ones, as granules are smaller and they can be more easily released. This observation also offers the possibility to develop a batch process by which nanocrystals with different crystalline types can be selectively isolated.

4. Conclusion

This study proposes, for the first time, an innovative solution against limitations of the current process for producing starch nanocrystals. Cross-flow filtration was proved to be an efficient continuous operation for separating SNC from the bulk suspension whatever the ceramic membrane pore size (0.2 μm–0.8 μm). Such proof of principle for this strategy, offers numerous opportunities for accelerating the potential industrialization of SNC. Indeed, it could improve (i) the yield of SNC preparation, (ii) the quality and homogeneity of SNC suspensions, and (iii) the ensuing final properties of composites/materials using SNC. Also, it is an industrial process proven to be effective, economical and energy saving compared to current isolation methods (centrifugation). Contrary to frontal filtration, cross-flow filtration allowed isolation without modifying the crystalline structure of SNC (and potentially isolate one type of crystallinity), nor favoring its aggregation.

Acknowledgements

Authors would like to thank Bertine Khelifi (Pagora) for her expertise in ESEM and FEGSEM imaging; and Nicolas Laudou from Pall France SAS (Scientific Laboratory, Saint Germain en Laye, France) for running the pilot tests. The research leading to these results has received funding from the European Community's Seventh Framework Programme (FP7/2007-2013) under grant agreement no 207810.

References

Angellier, H., Choisnard, L., Molina-Boisseau, S., Ozil, P., & Dufresne, A. (2004). Optimization of the preparation of aqueous suspensions of waxy maize starch nanocrystals using a response surface methodology. *Biomacromolecules*, *5*, 1545–1551.

Angellier, H., Molina-Boisseau, S., Dole, P., & Dufresne, A. (2006). Thermoplastic starch-waxy maize starch nanocrystals nanocomposites. *Biomacromolecules*, *7*(2), 531–539.

Angellier, H., Molina-Boisseau, S., & Dufresne, A. (2005). Mechanical properties of waxy maize starch nanocrystal reinforced natural rubber. *Macromolecules*, *38*(22), 9161–9170.

Angellier, H., Molina-Boisseau, S., & Dufresne, A. (2006). Waxy maize starch nanocrystals as filler in natural rubber. *Macromolecular Symposia*, *233*(1), 132–136.

Angellier, H., Molina-Boisseau, S., Lebrun, L., & Dufresne, A. (2005). Processing and structural properties of waxy maize starch nanocrystals reinforced natural rubber. *Macromolecules*, *38*(9), 3783–3792.

Angellier, H., Putaux, J.-L., Molina-Boisseau, S., Dupeyre, D., & Dufresne, A. (2005). Starch nanocrystal fillers in an acrylic polymer matrix. *Macromolecular Symposia*, *221*(1), 95–104.

Chen, G., Wei, M., Chen, J., Huang, J., Dufresne, A., & Chang, P. R. (2008). Simultaneous reinforcing and toughening: New nanocomposites of waterborne polyurethane filled with low loading level of starch nanocrystals. *Polymer*, *49*(7), 1860–1870.

Chen, Y., Cao, X., Chang, P. R., & Huneault, M. A. (2008). Comparative study on the films of poly(vinyl alcohol)/pea starch nanocrystals and poly(vinyl alcohol)/native pea starch. *Carbohydrate Polymers*, *73*(1), 8–17.

Cheryan, M. (1986). *Ultrafiltration handbook*. Lancaster, PA: Technomic Publishing.

Hinkova, A., Bohacenko, I., Bubnik, Z., Hrstkova, M., & Jankovska, P. (2004). Mineral membrane filtration in refinement of starch hydrolysates. *Journal of Food Engineering*, *61*(4), 521–526.

Hwang, K. J., & Huang, P. S. (2009). Cross-flow microfiltration of dilute macromolecular suspension. *Separation and Purification Technology*, *68*, 328–334.

Jane, J.-l., Wong, K.-s., & McPherson, A. E. (1997). Branch-structure difference in starches of A- and B-type X-ray patterns revealed by their Naegeli dextrins. *Carbohydrate Research*, *300*(3), 219–227.

Kristo, E., & Biliaderis, C. G. (2007). Physical properties of starch nanocrystal-reinforced pullulan films. *Carbohydrate Polymers*, *68*(1), 146–158.

Kumar, S. M., Madhu, G. M., & Roy, S. (2007). Fouling behaviour, regeneration options and on-line control of biomass-based power plant effluents using microporous ceramic membranes. *Separation and Purification Technology*, *57*(1), 25–36.

LeCorre, D., Bras, J., & Dufresne, A. (2010). Starch nanoparticles: A review. *Biomacromolecules*, *11*(5), 1139–1153.

LeCorre, D., Bras, J., Dufresne, A. (2011). Evidence of micro and nano-scaled particles during starch nanocrystals production and their isolation. *Biomacromolecules*. doi:10.1021/bm200673n.

Lin, N., Huang, J., Chang, P. R., Anderson, D. P., & Yu, J. (2011). Preparation, modification and application of starch nanocrystals in nanomaterials: A review. *Journal of Nanomaterial*, *13*, 13.

Master, A. M., & Steeneken, P. A. M. (1998). Filtration characteristics of maize and wheat starch hydrolysates. *Cereal Chemistry*, *75*(2), 241–246.

Pidgeon, E. F. (2009). *The application of crossflow membrane filtration to remediate wheat starch processing wastewater for reuse*. Griffith University.

Singh, N., & Cheryan, M. (1997). Fouling of a ceramic microfiltration membrane by corn starch hydrolysate. *Journal of Membrane Science*, *135*(2), 195–202.

Singh, N., & Cheryan, M. (1998a). Membrane technology in corn refining and bioproduct-processing. *Starch*, *50*(1), 16–23.

Singh, N., & Cheryan, M. (1998b). Process design and economic analysis of a ceramic membrane system for microfiltration of corn starch hydrolysate. *Journal of Food Engineering*, *38*(1), 57–67.

Viguié, J., Molina-Boisseau, S., & Dufresne, A. (2007). Processing and characterization of waxy maize starch films plasticized by sorbitol and reinforced with starch nanocrystals. *Macromolecular Bioscience*, *7*(11), 1206–1216.